Magnetic properties and thermal treatments in pseudobinary $TbPt_{1-x}Cu_x$ alloys

2003 J. Phys.: Condens. Matter 15 1339

(http://iopscience.iop.org/0953-8984/15/8/317)

INSTITUTE OF PHYSICS PUBLISHING JOURNAL OF PHYSICS: CONDENSED MATTER

J. Phys.: Condens. Matter **15** (2003) 1339–1351 PII: S0953-8984(03)56161-6

Magnetic properties and thermal treatments in pseudobinary $TbPt_{1-x}Cu_x$ alloys*

A Señas[1], J Rodríguez Fernández[1], J C Gómez Sal[1] and L Sánchez[2]

[1] DCITIMAC, Facultad de Ciencias, Universidad de Cantabria, Santander 39005, Spain
[2] DCITYM, ETSI de Caminos, Canales y Puertos, Universidad de Cantabria, Santander 39005, Spain

Received 15 November 2002
Published 17 February 2003
Online at stacks.iop.org/JPhysCM/15/1339

Abstract

The structural and magnetic properties of the $TbPt_{1-x}Cu_x$ orthorhombic compounds are studied in two series of samples: prepared 'as quenched' and after an annealing treatment. An extended analysis of the influence of the annealing in the microstructure of the samples was performed by x-ray, neutron diffraction and scanning electron microscopy. This analysis allows us to understand the modifications in the magnetic properties of both series, as a consequence of the sample homogenization process. Changes from ferromagnetism to antiferromagnetism with increasing Cu concentration are found in both series despite the ionic distance invariance. $x = 0.3$ is the composition limit between both behaviours. This study strongly supports the importance of the conduction band state rather than ionic distances in the magnetic behaviour of these rare earth–d compounds.

1. Introduction

In the rare-earth-based intermetallic compounds with a non-magnetic partner, direct magnetic exchange is negligible and the dominant magnetic interaction is of indirect type via conduction electrons. This is the case of the binary R–M compounds, where R is the rare earth and M is a d metal such as Ni, Cu, Pd, Ag, Pt, Au etc, when the d band is filled. The magnetic ordering in such compounds then stems from the Ruderman–Kittel–Kasuya–Yosida (RKKY) interaction, in which the exchange between R magnetic ions is mediated by the oscillating polarization of conduction electrons. The strength and sign of the long-range RKKY interaction strongly depends on the distance between the magnetic ions, $\boldsymbol{r}$, and the state of the conduction band, via the product $\boldsymbol{k}_F\boldsymbol{r}$, where $\boldsymbol{k}_F$ is the Fermi vector [1]. The original analytical form of this interaction was obtained assuming drastic simplifying approximations, such as perfectly free conduction electrons and a constant exchange integral of the local f–s (conduction electron) interaction. In spite of the unrealistic assumptions of the theory, it has been considered as the basis for an understanding of the interacting localized moments in metals due to its applicability

* This work is dedicated to professor Domingo González of the University of Zaragoza on his retirement.

in order to estimate the exchange constant and the effective mass and then to test the validity of the free electron approximation in some metals [2], and also for its successful accounting for some magnetic arrangements in simple cubic structures [3].

Considerable effort was made in the 1960s and 1970s to extend this theory to more realistic cases such as non-spherical Fermi surfaces [4] or making allowance for inter-electron interactions and particular forms of the f–s exchange integral [5]. However, in many cases, the improvements are not significant, and it is assumed that a proper realistic treatment of the indirect interaction is immensely complex, needing a real knowledge of the sub-band structure, which usually results in overlapping in the rare earth–transition metal compounds.

A common assumption of the RKKY model, in the analysis of the experimental results, has been to consider the rare earth distances as the most significant parameter which governs the change from ferro- to antiferromagnetism, recalling in an inadequate fashion the Bethe–Slater–Néel phenomenological curve. There is, however, no doubt as to the importance of the conduction band in determining the magnetic behaviour of these R–M alloys [6]. In particular, recent studies [7] highlight the crucial role of the density of states at the Fermi level, $n(E_F)$: ferromagnetism should be associated with large values of this parameter.

R–M alloys provide then an excellent scenario to analyse the origin and effects of the RKKY interactions. Some of these compounds are ferromagnetic (RNi, RPt, RPd, RZn and RGa) while others behave as antiferromagnets (RCu, RIn and RAg) [2, 8]. The study of the corresponding diluted compounds, $RM_xM'_{1-x}$, could show the evolution from one behaviour to the other. In this sense, a particularly relevant study is that carried out on the series $GdNi_{1-x}Cu_x$ and $GdPt_{1-x}Cu_x$ [9], in which a change in the magnetic character from ferro- to antiferromagnetism occurs with no volume variation for the second series and with a change of about 4% in the first one. These comparative results conclude that the role of the conduction electron in the magnetic interaction is relevant, since in both cases Cu provides additional electrons for the conduction band. Another interesting case is the $Ho_{1-x}Y_xNi$ series [10], which exhibits ferromagnetic behaviours for all the compositions in spite of the great variation of the interionic distance when increasing the Y content. Since Ho and Y contribute the same number of electrons to the conduction band, the substitution does not modify the ferromagnetic character of the samples, and only a decrease of T_C, proportional to the dilution percentage, was found as a consequence of the reduction of the average molecular field.

Gd compounds are, in principle, the best suited for this kind of study due to the absence of crystalline field effects. However, a proper determination of their magnetic structure is always difficult, due to the high absorption of Gd for neutron scattering, and the results are sometimes subject to controversy [11]. For this reason, we have undertaken a systematic study of the isomorphous series $TbPt_{1-x}Cu_x$; the expected high values of the Tb magnetic moments will facilitate our study. In addition, the comparison with the $TbNi_{1-x}Cu_x$ series [12], in which a change from ferro- to antiferromagnetism was observed for $x = 0.35$, will strengthen our discussion. TbPt (FeB-type structure) is ferromagnetic with $T_C = 56$ K [13], while TbCu (CsCl-type structure) presents an antiferromagnetic behaviour with $T_N = 118$ K and a martensitic transition to the FeB structure at low temperatures [14]. The corresponding Néel temperature of the FeB structure is $T_N = 47$ K [15].

The aim of this work is twofold: on the one hand, to study the crystalline structure of the series regarding its preparation processes, with a careful determination of the evolution of some crystalline parameters (cell parameters and interionic distances through the series); on the other hand, to determine the magnetic properties of the series, confronting the effects of thermal treatments on these properties. The comparison with the parent $TbNi_{1-x}Cu_x$ series is also considered in the discussion.

2. Experimental details

Two series of polycrystalline samples of $TbPt_{1-x}Cu_x$ were prepared by arc-melting stoichiometric amounts of high purity constituents under argon atmosphere. These preliminary metals were melted with special care in order to avoid the loss of some of the components as a consequence of the initial melting reaction, and subsequently no total weight losses were detected after this process. Once the first ingot had been obtained, the melting procedure was repeated five times in order to get a good mixture of all the components and a overall homogeneity in the sample. The cooling time was not higher than a few seconds.

The first series, named 'as quenched' (AQ), and prepared as explained above, corresponds to samples with compositions $x = 0, 0.2, 0.3, 0.4, 0.6, 0.8$ and 1. A second series was prepared in the same way, and afterwards subjected to thermal treatments. A high vacuum annealing at 750 °C (below the melting point) for 1 week was carried out in the samples with compositions $x = 0, 0.1, 0.2, 0.3, 0.4, 0.5, 0.6$ and 0.7, constituting the series named 'annealed' (AN). The annealing procedure will enhance the homogeneity of the samples.

Samples were prepared for scanning electron microscopy (SEM) observations by using grinding paper discs in grain sizes of 100, 240, 600 and 1000 mesh and final polishing with diamond paste. The SEM images were produced with a JEOL electron microscope, model JSM 5800LV, equipped with an Oxford Link energy-dispersive spectrometer, model eXL, at the University of Cantabria. Zooms between 300 and 2500 were reached, and quantitative electron probe microanalysis (EPMA) techniques were used to verify the chemical composition of the phases.

Magnetic measurements were performed at the Magnetism Laboratory, University of Cantabria, using a PPMS (Quantum Design) device from 1.8 to 300 K in applied fields up to 9 T.

The crystalline structures were determined by x-ray and neutron diffraction experiments. Neutron diffraction experiments down to 1.5 K were performed both at G4.1 (Laboratoire Lèon Brillouin, France) and D1.B (Institute Laue–Langevin, France) using wavelengths of 2.4266 and 2.5239 Å, respectively. Analyses were held by Rietveld refinement methods, using the program Fullprof [16].

3. Crystallography

The crystalline structures of the $TbPt_{1-x}Cu_x$ compounds have been determined by x-ray diffraction at 300 K, and by neutron diffraction at lower temperatures. All the studied compounds in both series, with $x < 1$, crystallize in the FeB-type structure, *Pnma* space group (no 62). No other extra phases were detected, except for the AQ $TbPt_{0.2}Cu_{0.8}$ compound, for which 12% of the cubic TbCu phase was found at 300 K. We have, therefore, discarded this compound for any kind of deeper analysis.

In the AQ series, the narrowness of the peaks seemed to guarantee the good crystallization of the samples. Only small changes in the peaks' widths and slight modifications in the cell parameters were induced by the annealing process. In figure 1, we compare the two x-ray spectra for the AQ and AN $TbPt_{0.8}Cu_{0.2}$ compound at 300 K, as an example. In table 1, the crystallographic data at 300 K of both series are presented. As can be observed, despite the similar aspects of the AQ and AN patterns, the Bragg factor is notably improved in the AN series. The analysis of the lowest temperature spectra (1.5 K) allows us to determine the relative volume variation, $\Delta V/V$, giving us values of 4.5×10^{-3} for the AQ series, and 6×10^{-3} for that of AN, very similar to those obtained in other rare earth intermetallics [17].

The most striking result is the fact that the Pt/Cu substitution does not induce appreciable changes in the cell volume ($\approx$0.4% in both series). In figure 2, we compare the volume variation

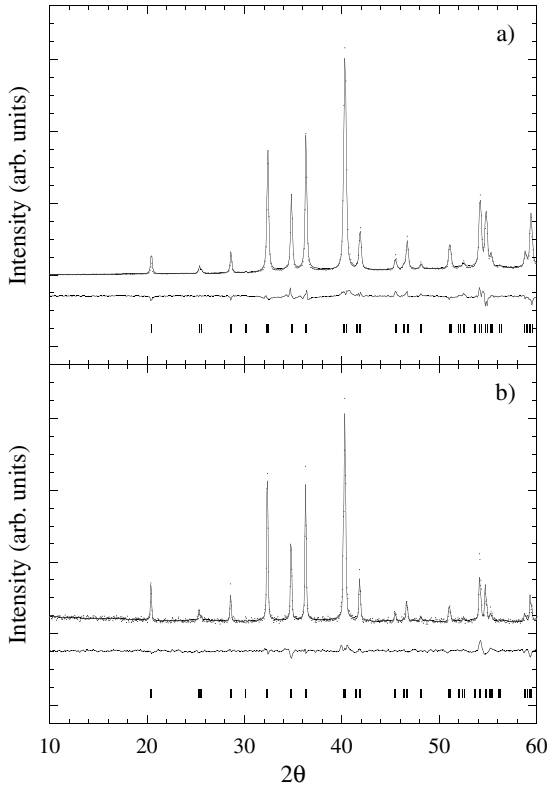

Figure 1. X-ray diffraction spectra of the (a) AQ and (b) AN $TbPt_{0.8}Cu_{0.2}$ at 300 K. The vertical marks represent the positions of the Bragg peaks, and the curves at the bottom correspond to the difference pattern between the observed and calculated intensities.

Table 1. Crystallographic data of the (a) AQ and (b) AN $TbPt_{1-x}Cu_x$ series obtained by means of x-ray diffraction at 300 K.

	(a) AQ $TbPt_{1-x}Cu_x$					(b) AN $TbPt_{1-x}Cu_x$				
x	a (Å)	b (Å)	c (Å)	V (Å^3)	R_{Bragg} (%)	a (Å)	b (Å)	c (Å)	V (Å^3)	R_{Bragg} (%)
0	7.0121(4)	4.4911(3)	5.5563(4)	174.98	17					
0.2	7.0288(5)	4.4859(4)	5.5423(5)	174.75(2)	23	7.0279(3)	4.4858(2)	5.5407(2)	174.67(1)	13
0.3	7.0445(6)	4.4834(5)	5.5370(5)	174.88(2)	19	7.0416(6)	4.4820(4)	5.5331(5)	174.63(3)	12
0.4	7.0609(5)	4.4826(4)	5.5294(4)	175.01(2)	18	7.0671(4)	4.4722(4)	5.5273(3)	174.69(2)	17
0.5						7.0848(4)	4.4711(3)	5.5185(3)	174.81	12
0.6	7.0928(9)	4.4759(6)	5.5133(6)	175.03(4)	25	7.1009(4)	4.4681(3)	5.5093(3)	174.79(1)	15
0.7						7.111(2)	4.4748(9)	5.495(1)	174.84	12

versus Cu content in the $TbPt_{1-x}Cu_x$ series and in the isomorphous $TbNi_{1-x}Cu_x$, in which a volume increase of about 4.5% was found [18]. The volume invariance in the Pt-based series is achieved due to a slight increase in the 'a' parameter, and small decreases in the 'b' and 'c' parameters, with increasing Cu concentration. This leads to a non-significant modification in the R–R or R–M nearest neighbours' distances.

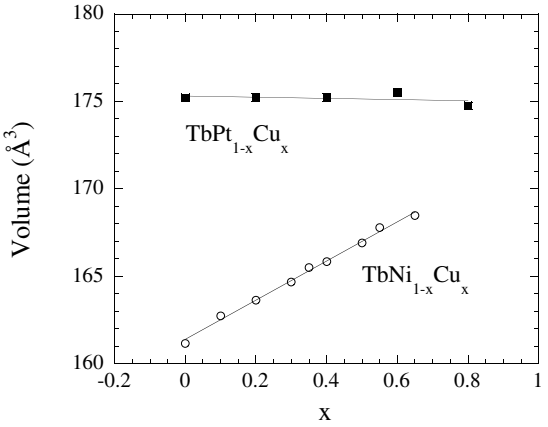

Figure 2. Cell volume of the compounds $TbPt_{1-x}Cu_x$ and $TbNi_{1-x}Cu_x$ at 300 K.

X-ray and neutron diffraction in powdered samples will never provide us with more than an average analysis. In order to obtain a deeper knowledge of the metallurgy and microstructure of the samples, we have also performed a SEM study.

Due to its speed and simplicity, the energy-dispersive spectrometer, EDS, is the most common x-ray measurement instrument to be found on an electron microscope. As well as identifying which elements are present in the sample, EDS can also tell how much, and where the elements are distributed. We have prepared samples from an ingot cut into slices, thereby always obtaining similar images. Then, although EDS is a surface technique, the information obtained in this way could be considered as representative of the bulk material. Therefore, the obtained backscattered electron (BSE) images provide us with semi-quantitative data about composition homogeneity in a sample. The BSE images of the AQ $TbPt_{1-x}Cu_x$ samples revealed that most of their volumes consist of little dendrites with a high contrast central area, which corresponds to Pt-rich $TbPt_{1-x}Cu_x$ concentrations, separated by darker Cu-rich intergranular regions, giving variations in x of about 20% on the scale of 10 μm. A thermal treatment is then suggested to eliminate the 'cored' structure in the AQ samples. In fact, this segregation with concentration gradients across the grains due to the high cooling rates in the AQ melting procedure is far from being the most suitable, and atomic diffusion processes are desirable to obtain compositionally homogeneous grains. EPMA measurements revealed that, in our case, the AN samples are completely homogeneous and only a few impurities (<3% in total) of elemental Cu, pure Tb and $TbCu_2$ were detected. This is illustrated in figure 3, in which we compare the BSE images of the nominal compound $TbPt_{0.6}Cu_{0.4}$ as quenched (a) and after the annealing process (b). On the scale of 10 μm, concentrations of about 47% $TbPt_{0.7}Cu_{0.3}$ and 44% $TbPt_{0.5}Cu_{0.5}$ were found in the AQ sample providing a dendrite-like image as described. In contrast, the AN sample is homogeneous in all regions that were scanned with a global volume of 97.5% of a single $TbPt_{0.6}Cu_{0.4}$ phase. Some of the black dots are $TbCu_2$ in concentrations of about 2.5%, whereas the others are due to holes appearing in the bulk material.

Taking into account the differences between the melting points of TbPt and TbCu pure phases, it is clear that a long-enough annealing process favours the dilution of the Pt-rich and Cu-rich phases, homogenizing the sample. Diffraction methods do not discriminate the different compositional phases observed in the AQ series because there are no significant changes in the cell parameters, and then microstructural information of these samples and the effect of the annealing processes must be obtained from electron microscopy.

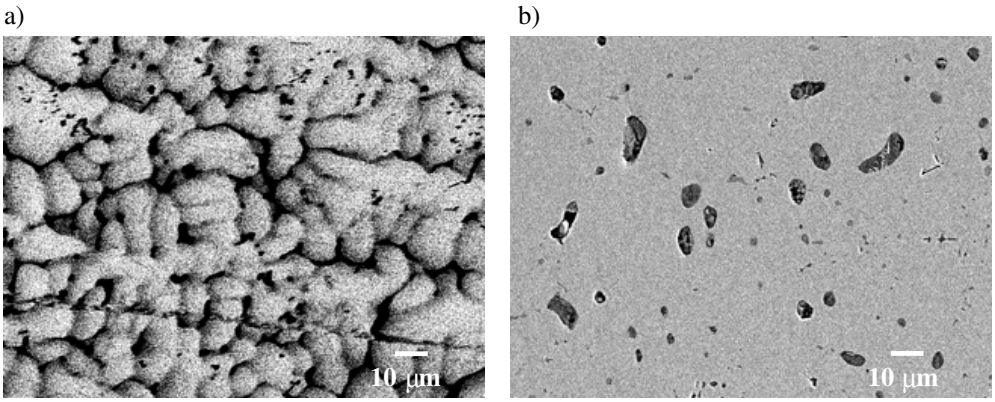

Figure 3. SEM images of the (a) AQ and (b) AN $TbPt_{0.6}Cu_{0.4}$. It can be observed how the granular structure relaxes after the annealing at 750 °C, providing a homogeneous image with some sprinkled holes and impurities of $TbCu_2$.

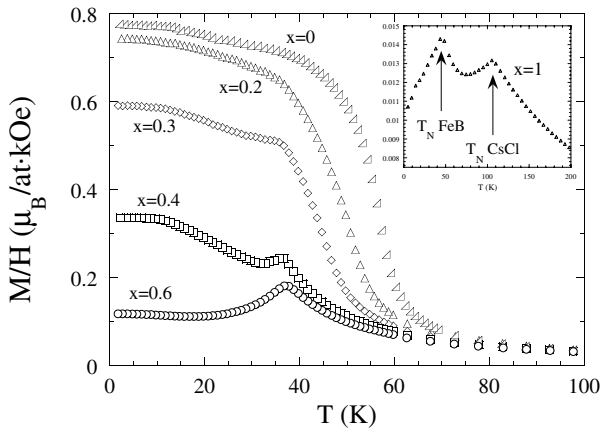

Figure 4. Thermal variation of the magnetization of the AQ series $TbPt_{1-x}Cu_x$ under a constant magnetic field of 2 kOe. The curve corresponding to TbCu is shown in the inset.

4. Magnetic measurements

4.1. 'As-quenched' series

The susceptibility versus temperature curves in a constant magnetic field of 2 kOe for the compositions of the AQ $TbPt_{1-x}Cu_x$ series are presented in figure 4. The $x = 0$ and 0.2 compounds present a clear ferromagnetic behaviour. In this figure, there can also be observed a progressive decrease of the susceptibility (magnetization) values with increasing Cu content, x. Simultaneously, an anomalous peak at 36.5 K appears superimposed on the main ferromagnetic behaviour in the dilutions, and becomes more intense for higher x values. This peak is characteristic of antiferromagnetism. Then, all the compounds with $x \geqslant 0.6$ can be considered as antiferromagnetic. TbCu, presented in the inset of figure 4 on a larger scale, shows a clear antiferromagnetic behaviour, in which the two maxima correspond to the Néel temperatures of the CsCl and FeB structures, appearing through the martensitic transformation [14, 15].

Table 2. Magnetic properties of the AQ $TbPt_{1-x}Cu_x$ series. H_C means the critical or metamagnetic field for FM or AFM compounds respectively, as explained in the text.

x (Cu)	T_C (K)	T_N (K)	θ_P (K)	μ_{eff} (μ_B)	T_W (K) at 200 Oe	H_C (kOe) at 5 K	M (μ_B) at 5 K and 90 kOe
0	56		38.2	9.8			6.47
0.2	47		33.5	9.79	12	1.2	6.00
0.3	∼45	36.5	32.2	9.83	12	0.9	4.47
0.4	∼38	36.5	31.4	9.62	5	∼0.5	6.02
0.6		36	22.0	9.84		7.5	5.68
1		116/47.5	−54	9.79			

The ordering temperatures, determined at the inflexion point of the M/H curves for the ferromagnetic compounds and at the maximum on the susceptibility curves for the antiferromagnets, are listed in table 2. As can be observed, the Curie temperature of the FM compounds decreases with increasing Cu content, while the Néel temperature of the AFM compounds remains almost constant except for TbCu (with a different crystalline structure).

A Curie–Weiss law is obtained for all the compounds at temperatures above 100 K. Deviations of this law close to the ordering temperatures are due to crystal field effects. The effective magnetic moment is close to the expected free ion value of Tb^{3+} ($\mu_{eff} = 9.72\ \mu_B$) corresponding to the $^7F_6$ ground state level. The paramagnetic Curie temperatures (θ_P) decrease with increasing Cu content, reaching negative values for the compound TbCu, indicating the progressive enhancement of the negative interactions.

In figure 5, we present the low temperature regime in the magnetization measured in a 200 Oe field after a zero-field cooling (ZFC) and after cooling under a constant 200 Oe applied magnetic field (FC), for the ferromagnetic $TbPt_{0.8}Cu_{0.2}$ compound and for $TbPt_{0.6}Cu_{0.4}$, with a marked anomaly at 36.5 K. In both cases, a thermomagnetic irreversibility is observed. Such behaviour in ferromagnetic compounds with strong magnetocrystalline anisotropy is due to the existence of narrow domain walls, and has been described in several other low symmetry rare earth compounds [19, 20]. T_W corresponds to the temperature at which the applied magnetic field of 200 Oe is large enough to drive the domain wall motion. Obviously, for antiferromagnetic arrangements, the narrow wall motion effects cannot appear. This is well illustrated in the behaviour of the $x = 0.4$ compound (figure 5), in which no irreversibility is observed in the maximum corresponding to the antiferromagnetism, but does appear in the ferromagnetic contribution with an estimated T_W around 5 K. This demonstrates the superposition of two contributions in our AQ samples. The percentage of each one evolves with x from pure ferromagnetism in TbPt to pure antiferromagnetism in TbCu.

In figure 6, we show the magnetization curves at different temperatures for applied fields up to 9 T for the compounds $TbPt_{0.8}Cu_{0.2}$ (FM) and $TbPt_{0.4}Cu_{0.6}$ (AFM). In the inset of figure 6(a), the low field region of the $M(H)$ curves is shown. The critical field H_C again reflects the narrow wall motion phenomena. A critical H_C field estimated at around 1200 Oe corresponds to the wall motion field at 5 K. At 10 K the H_C field is about 600 Oe, and above 30 K the transition is not appreciable. We can observe that the magnetization remains unsaturated for both samples even at high magnetic applied fields, which is again explained due to the strong magnetocrystalline anisotropy of these compounds. For $TbPt_{0.4}Cu_{0.6}$, a metamagnetic transition at 7.5 kOe and 5 K was found. This critical field, which decreases when temperature increases and disappears above the Néel temperature, is also present for the other AFM compounds in this series.

All the characteristic magnetic values are presented in table 2.

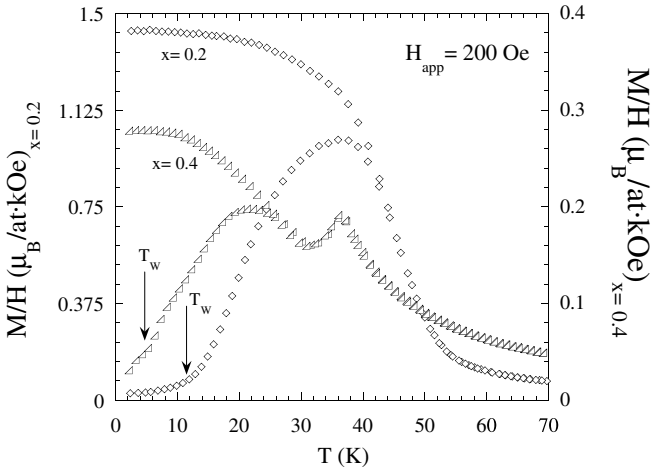

Figure 5. Field-cooled and zero-field-cooled measurements for the AQ $TbPt_{0.8}Cu_{0.2}$ and $TbPt_{0.6}Cu_{0.4}$ under a constant magnetic field of 200 Oe.

4.2. Annealed series

In figure 7, we present the susceptibility versus temperature in a constant magnetic field of 2 kOe for the AN studied compounds. A rapid inspection of this figure denotes remarkable changes with respect to the variation obtained in the AQ samples (see figure 4). These changes merit a careful analysis.

Two kinds of behaviour, figures 7(a) and (b), are clearly observed. In figure 7(a), ferromagnetic behaviours are found for $x = 0$, 0.1 and 0.2. The step in the magnetization of TbPt has already been detected in a previous characterization [13] and it was attributed to a reorientation of a particular sublattice of magnetic moments [21]. The M/H versus T curve of $x = 0.3$ shows a ferromagnetic behaviour below 23.1 K, which evolves into antiferromagnetic at higher temperatures, defining a $T_N = 36.9$ K. In contrast to the AQ case, for the AN sample it is not a superposition of both behaviours that we observe (FM and AFM), but a complete temperature-induced change from one to the other. This is supported not only by the high values at low temperatures of the M/H curves, which are comparable to those obtained for $x = 0$, 0.1 and 0.2, but also by neutron diffraction measurements [22]. Then, the $x = 0.3$ compound corresponds to the limit between the ferro and antiferromagnetic behaviours.

In figure 7(b), we present the compounds with a clear antiferromagnetic behaviour, with well defined Néel temperatures. Small traces of a possible ferromagnetic phase are detected especially in $x = 0.5$. The main magnetic characteristics of these samples are presented in table 3. A comparison with values given in table 2 reveals slight changes in the ordering temperature values and a weak increase in the paramagnetic Curie temperatures, θ_P, after thermal treatments. However, the values of the effective magnetic moments are slightly reduced with respect to the effective magnetic moment of the free ion of Tb^{3+} ($\mu_{eff} = 9.72\,\mu_B$), quite clearly due to conduction band effects [23, 24], which stand out clearly once we have eliminated the phases' coexistence upon the annealing processes.

Figure 8 shows the magnetization curves for the $x = 0.2$ and 0.6 compounds. The noticeable new features with respect to the AQ samples (see figure 6) are the following. The field transition already mentioned for the AN TbPt is also observed in the ferromagnetic $x = 0.2$ composition at 5 and 30 K. This indicates that for the ferromagnetic compounds with $x = 0.1$

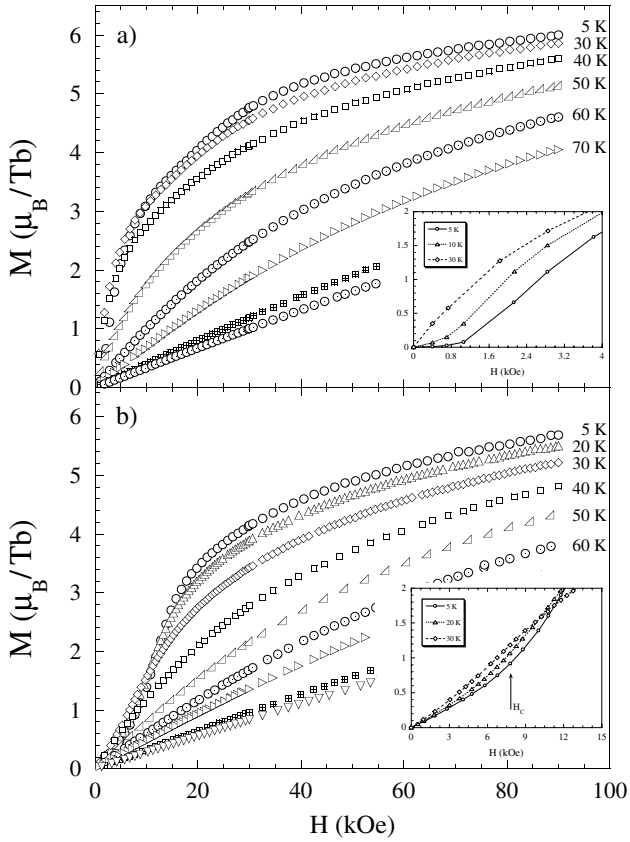

Figure 6. Magnetization curves of the AQ (a) $TbPt_{0.8}Cu_{0.2}$ and (b) $TbPt_{0.4}Cu_{0.6}$ at several temperatures between 5 and 100 K. In the inset of both figures, the low field region at low temperatures is shown.

Table 3. Magnetic properties of the AN $TbPt_{1-x}Cu_x$ series. H_C means the critical or metamagnetic field for an FM or AFM compound, respectively, as explained in the text.

x (Cu)	T_C (K)	T_N (K)	θ_P (K)	μ_{eff} (μ_B)	T_W (K) at 200 Oe	H_C (kOe) at 5 K	M (μ_B) at 5 K and 90 kOe
0	57.7		39.4	9.48			
0.1	54.5		39.3	9.55	11	1.2	5.83
0.2	46.8		35.4	9.58	14	1.5	5.66
0.3	23.1	36.9	33.2	9.52	7	0.9	5.55
0.4		36.8	31.4	9.46			
0.5		35.7	32.8	9.60		7.9	5.72
0.6		36.7	33.1	9.56		5.4	5.78
0.7		36.1	23.5	9.60		4.5	5.11

and 0.2, the magnetic structure should be the same, ferromagnetic and non-collinear, as that found in TbPt, being at the origin of such steps in the magnetization curves. The effects of narrow wall motion are also observed in the low field regions of the ferromagnetic AN samples. For $TbPt_{0.4}Cu_{0.6}$, the metamagnetic transition becomes more abrupt than in the AQ sample

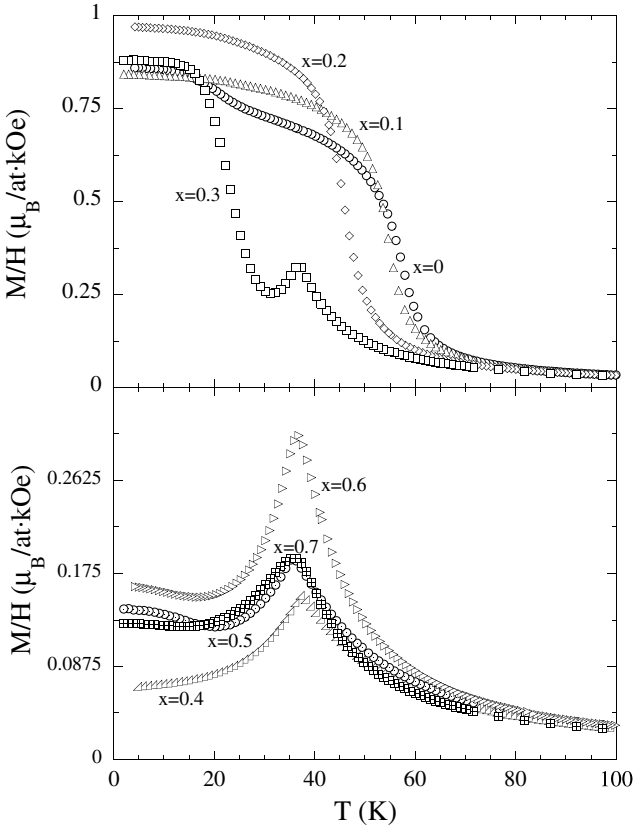

Figure 7. Thermal variation of the magnetization of the AN $TbPt_{1-x}Cu_x$ series under a constant field of 2 kOe.

and takes place at a lower field, 5.4 kOe at 5 K, as a consequence of the global homogenization of the sample, which now presents a unique composition.

5. Discussion and conclusions

We have investigated the effect of different synthesis methods (in particular, arc furnace melting and further thermal annealing) upon the structural and magnetic properties of polycrystalline $TbPt_{1-x}Cu_x$ compounds.

A mere characterization with diffraction methods (x-ray and neutrons) gave us the correct crystalline structure for the AQ samples and non-significant modifications appear in the diffraction patterns of the AN ones, due to the average character of these methods. However, it has been detected via SEM imaging that notable differences appear in the granular microstructure of the samples. In particular, the AQ samples could be understood as a weighted mixture of different phases, a Pt-rich one in the grains' core and the other a Cu-rich intergranular one, giving a correct average nominal composition. This particular microstructure appears due to the large differences between the fusion temperatures of TbCu (900 °C) and TbPt (1500 °C), inducing the phase segregation processes. The annealing favours the atomic diffusion, and leads to a homogenization of the samples, reaching a unique phase corresponding to the nominal composition.

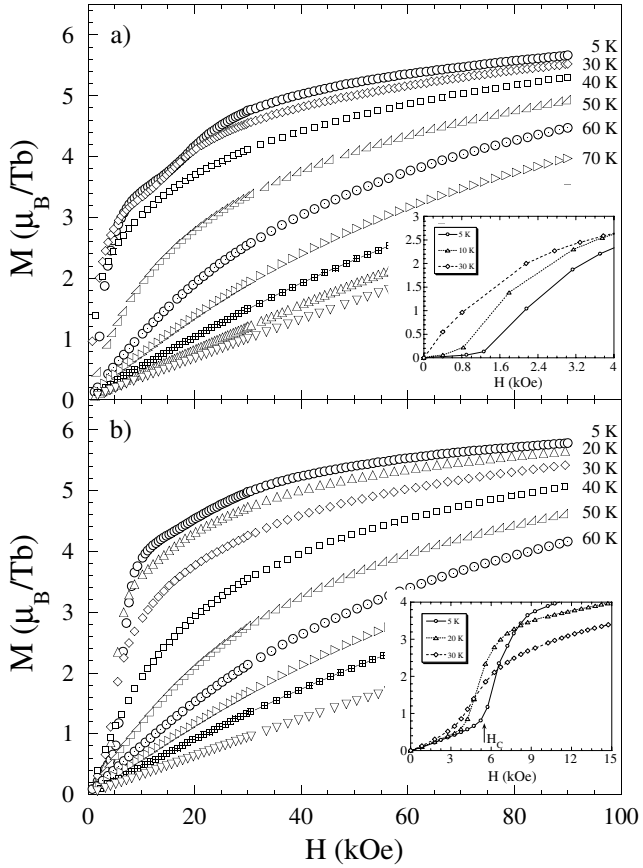

Figure 8. Magnetization curves of the AN (a) $TbPt_{0.8}Cu_{0.2}$ and (b) $TbPt_{0.4}Cu_{0.6}$ at several temperatures between 5 and 100 K. In the inset of both figures, the low field region at low temperatures is shown.

The understanding of the effects of thermal treatments elucidates the observed magnetic behaviours. In figure 9, we compare the AQ and AN thermal variation of the susceptibility for two significant compositions. For the $TbPt_{0.6}Cu_{0.4}$ sample, figure 9(a), the annealing process progressively removes the ferromagnetic Pt-rich phase and a one week annealing process provides a unique antiferromagnetic phase, corresponding to the nominal $TbPt_{0.6}Cu_{0.4}$ composition.

More significant is the behaviour of the $TbPt_{0.7}Cu_{0.3}$ sample, see figure 9(b), in which the annealing processes lead to a unique phase with the already mentioned thermal evolution from AFM to FM, while the AQ sample denotes the mere superposition of ferro and antiferromagnetic behaviours corresponding to the two segregated phases. Recent neutron diffraction experiments [22] at low temperatures in the AQ samples confirmed the coexistence of FM and AFM magnetic structures, which are individually associated with those of nominal compositions obtained in the AN samples.

As occurs in many other RMM′ [25–27] systems, the introduction of Cu modifies the conduction electron concentration and gives rise to an enhancement of the negative magnetic interactions. The most remarkable feature of these Pt/Cu substitutions is that the evolution from ferromagnetism to antiferromagnetism takes place with negligible volume and atomic distance

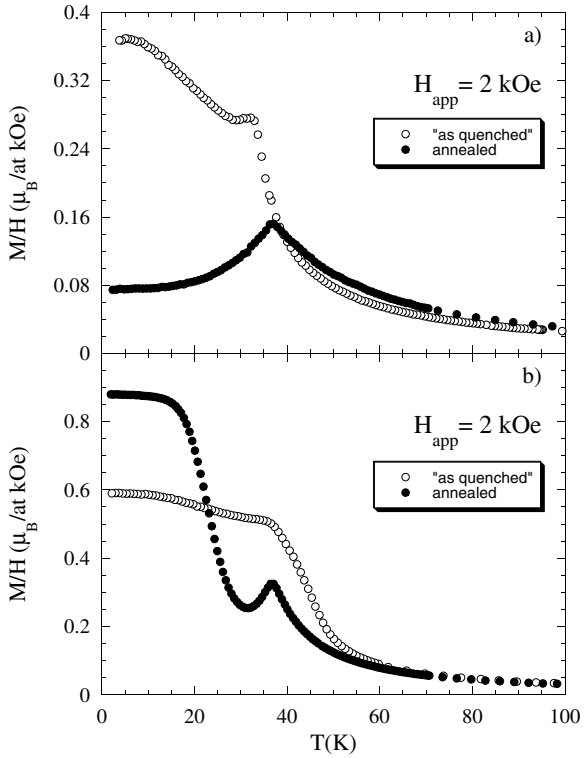

Figure 9. Compared magnetization of the AQ and AN (a) $TbPt_{0.6}Cu_{0.4}$ and (b) $TbPt_{0.7}Cu_{0.3}$ under a constant field of 2 kOe.

variations through the series. The magnetic change occurs for a Cu content of about 30% in the AN series. A similar evolution has been found for the series $TbNi_{1-x}Cu_x$ [12]. In this last case, the magnetic change appears for a Cu concentration of 35% as volume increases by about 4.3% (see figure 2). In both cases, the Cu introduction on the Pt/Ni sites modifies the number of conduction electrons, while the substitution by another element of the same Ib column of the periodic table, such as Ag, does not modify this parameter, and then the magnetic behaviour remains unchanged. TbCu and TbAg present the same type of antiferromagnetic structure [28]. In this sense, TbNi [19] and TbPt [13] are both ferromagnets, Ni and Pt being in the same column. All these results strongly support the fact that it is not the mean distances between the magnetic ions which control the magnetism of these compounds. It is clear that the FM–AFM change is due to the modifications on the conduction band as a result of the Cu substitutions. Furthermore, the study performed in the isomorphous series $Gd(Pt/Ni)_{1-x}Cu_x$ [9], with an $L = 0$ Gd state, reveals the same behaviour as the Tb-based series described in this paper, discarding any influence of the magnetocrystalline anisotropy in the observed evolution of the magnetic properties. The importance of the conduction band to control the magnetic character of metallic compounds, in particular the crucial role of the density of states at the Fermi level, $n(E_F)$, is the main conclusion supported in recent articles [7, 29, 30]. In fact, these authors claim that the sign of the indirect long range magnetic interactions is governed by the value of $n(E_F)$, assuming that the free electron picture (spherical Fermi surfaces) is not the correct description. This seems to be the case, at least, in these low symmetry rare earth compounds with non-magnetic partners, where the conduction band is solely the transport medium of the magnetic interactions.

Neutron diffraction under pressure and XPS experiments have been undertaken in order to obtain further support of these conclusions.

Acknowledgments

This work has been supported by the Spanish CICYT under the project MAT 99-0667-C04-01.

We acknowledge the help in neutron diffraction measurements of Gilles André at LLB (G4.1) and Javier Campo at ILL (D1.B).

References

[1] See for instance
Coqblin B 1977 *The Electronic Structure of Rare-Earth Metals and Alloys: the Magnetic Heavy Rare-Earth* (London: Academic)
Jensen J and Mackintosh A R 1991 *Rare Earth Magnetism: Structures and Excitations* (New York: Oxford University Press)
[2] Kirchmayr H R and Poldy C A 1979 *Handbook on the Physics and Chemistry of Rare Earths* vol 1, ed K A Gschneidner Jr and L Eyring (Amsterdam: North-Holland) ch 14
[3] Sakurai J, Kubo Y, Kardo T, Pierre J and Bertaut E F 1973 *J. Phys. Chem. Solids* **34** 1305–16
[4] Roth L M, Zeiger H J and Kaplan T A 1966 *Phys. Rev.* **149** 519
[5] Debray D K and Sakurai J 1974 *Phys. Rev.* B **9** 2129
[6] Campbell I A 1972 *J. Phys. F: Met. Phys.* **2** L47
[7] Hernando A, Rojo J M, Gómez Sal J C and Novo J M 1996 *J. Appl. Phys.* **79** 4815
[8] Fournier J M and Gratz E 1993 *Handbook on the Physics and Chemistry of Rare Earths* vol 17, ed K A Gschneidner Jr, L Eyring, G H Lander and G R Choppin (Amsterdam: North-Holland) ch 115 Lanthanides/Actinides: Physics—I
[9] Rubio Temprano D, Rodríguez Fernández J, Gómez Sal J C, Hernando A and Rojo J M 1999 *J. Magn. Magn. Mater.* **196/197** 770–2
[10] Blanco J A, Rodríguez Fernández J, Gómez Sal J C, Rodríguez Carvajal J and Gignoux D J 1995 *Phys. Condens. Matter* **7** 2843
[11] Blanco J A, Gómez Sal J C, Rodríguez Fernández J, Castro M, Burriel R, Gignoux D and Schmitt D 1994 *Solid State Commun.* **89** 389–92
[12] Gignoux D and Gómez Sal J C 1976 *J. Magn. Magn. Mater.* **1** 203–13
[13] Castets A, Gignoux D and Gómez Sal J C 1980 *J. Solid State Chem.* **31** 197–207
[14] Ibarra M R, Chien T S and Pavlovic A S 1989 *J. Less Common Met.* **153** 233
[15] Señas A, Espeso J I, Rodríguez Fernández J, García Soldevilla J, Gómez Sal J C, Rodríguez Carvajal J and Ibarra M R 2000 *Physica* B **276–278** 614–15
[16] Rodríguez-Carvajal J 1993 *Physica* B **192** 55
[17] Espeso J I, Rodríguez Fernández J, Gómez Sal J C and Blanco J A 1994 *IEEE Trans. Magn.* **30** 1009
[18] Gignoux D 1973 *PhD Thesis* University of Grenoble, CNRS A0 no 8244
[19] Gignoux D 1974 *J. Physique* **35** 455
[20] Garcia-Soldevilla J, Gómez Sal J C, Rodríguez Fernández J, Espeso J I and Argüelles M A 1998 *J. Magn. Magn. Mater.* **186** 49–55
[21] Gignoux D and Lemaire R 1974 *Solid State Commun.* **14** 877
[22] Señas A 2003 *PhD Thesis* Universidad Cantabria
[23] Buschow K H J 1980 *Ferromagnetic Materials* vol 1, ed E P Wohlfarth (Amsterdam: North-Holland) ch 4 p 297
[24] Szytula A 1991 *Handbook of Magnetic Materials* vol 6, ed K H J Buschow (New York: Elsevier) ch 2 p 85
[25] Blanco J A, Gómez Sal J C, Rodríguez Fernández J, Gignoux D, Schmitt D and Rodríguez-Carvajal J 1992 *J. Phys.: Condens. Matter* **4** 8233
[26] Takei K, Ishikawa Y, Watanabe N and Tajima K 1979 *J. Phys. Soc. Japan* **47** 888
[27] Van Dongen J C, Palstra T T M, Morgownik A F J, Mydosh J A, Geerken B M and Buschow K H J 1983 *Phys. Rev.* B **27** 1887
[28] Cable J W, Koehler W C and Wollen E O 1964 *Phys. Rev.* A **136** 1240
[29] Fontcuberta J, Seffar A, Hernando A, Gómez Sal J C and Rojo J M 1997 *J. Appl. Phys.* **81** 3887
[30] Hernando A, Barandiarán J M, Rojo J M and Gómez Sal J C 1997 *J. Magn. Magn. Mater.* **174** 181